ELSEVIER

Cement & Concrete Composites 25 (2003) 311–319

Cement & Concrete Composites

www.elsevier.com/locate/cemconcomp

Mechanically pulped sisal as reinforcement in cementitious matrices

H. Savastano Jr. [a,*], P.G. Warden [b], R.S.P. Coutts [c]

[a] University of São Paulo, P.O. Box 23, 13635-900 Pirassununga SP, Brazil
[b] CSIRO Forestry and Forest Products, Private Bag 10, Clayton South, Vic., 3169, Australia
[c] ASSEDO Pty Ltd., 75 Sandringham Road, Sandringham, Vic., 3191, Australia

Received 26 February 2001; accepted 3 July 2002

Abstract

The performance as reinforcement of fibres obtained from commercial and by-product sisal (*Agave sisalana*) by thermomechanical pulping and chemi-thermomechanical pulping (CTMP) processes was investigated. Ordinary Portland cement (OPC) and chemically activated blast furnace slag (BFS) were examined as binders. The flexural strengths of OPC- and BFS-based composites incorporating 8% fibre reinforcement by mass were similar at 28 days and ranged from 18 to 22 MPa. Corresponding modulus of elasticity values were in the region of 11 GPa for the OPC-based composites and 7 GPa for the BFS-based composites. Water absorption values at 8% fibre content lay in the range of 21–31% by mass and density values in the region of 1.5 g/cm^3. Fracture toughness increased with fibre content, reaching a value of 1.6 kJ/m^2 at a content of 12% in the case of by-product sisal CTMP in the BFS matrix. Scanning electron microscopy provided interfacial bonding information that can be related to the mechanical performance of these fibre-reinforced pastes.

Keywords: Alternative fibre–cements; Vegetable fibres; Clinker-free cement; Microscopy

1. Introduction

Vegetable fibres from non-wood plants constitute abundant and low-cost raw-materials in many developing countries [1]. Several fibres show promise for utilisation as reinforcement in composite building materials. Success in a broad field of applications can be influenced by the choice of fabrication method and its ability to capture the optimum performance of the cellulose fibres [2]. It is also dependent on overcoming major concerns relating to fibre degradation in cementitious media [3].

The present study was carried out in an attempt to produce a viable fibre–cement material using the Hatschek method and non-conventional mechanical pulps of sisal (*Agave sisalana*) as reinforcement. A clinker-free binder based on ground blast furnace slag (BFS) was chosen for testing because of its availability at affordable prices and its low alkalinity [4] in comparison with ordinary Portland cement (OPC).

Mechanical pulps can provide adequate reinforcement in air-cured wood fibre–cement products [5] and are cheaper than conventional chemical pulps (e.g. kraft). Mills producing mechanical pulps are economically viable at a smaller scale of production and their effluents are less troublesome for treatment and disposal. Frictional energy is used in mechanical pulping as the principal means of achieving both fibre separation and fibrillation.

The use of pulped fibres and a slurry de-watering/pressure compaction process for the production of thin panels results in a predominantly two-dimensional (2D) and homogeneous distribution of the fibres in the matrix. This approach also results in improved fibre–matrix bonding and hence greater reinforcing efficiency when compared with the use of vegetable fibres in strand form. The use of such microfibres results in better fibre packing and thus higher fibre volume fractions (as much as 10%) are obtainable, resulting in significant increases in flexural strength and toughness [6–8].

The lignin and hemicellulose components of natural fibres can be chemically degraded in the highly alkaline environment of OPC [3,9]. Cement matrices of lower alkalinity are less aggressive and the use of BFS, partial

* Corresponding author. Fax: +55-19-5611689.
E-mail address: holmersj@usp.br (H. Savastano Jr.).

0958-9465/03/$ - see front matter
PII: S0958-9465(02)00055-0

substitution of clinker by pozzolanic material and accelerated carbonation are known means of improving the durability of vegetable fibre reinforcement [10,11].

2. Experimental work

This study was developed at the Commonwealth Scientific and Industrial Research Organisation (CSIRO), Division of Forestry and Forest Products (FFP), Australia, as part of a collaborative work with the University of São Paulo (USP), Brazil.

2.1. Binders

Adelaide Brighton brand OPC, Type GP (Australian Standard AS 3972-1991), was used as a reference binder. Basic granulated iron BFS provided by Companhia Siderúrgica Tubarão (CST), Brazil, and fully characterised by Oliveira et al. [4], was ground to an average Blaine fineness of 500 m^2/kg and employed as the main component of an alternative binder. Ground natural gypsum and construction grade hydrated lime (Australian Standard AS 1672) were added as activators in the proportions of 0.88:0.10:0.02 (BFS:gypsum:lime) by mass, as suggested by John et al. [12].

2.2. Fibre preparation and characterisation

Mechanically combed commercial sisal slivers approximately 2.5 m in length were provided by Geo. Kinnear and Sons Pty Ltd, Melbourne, Australia. Strands approximately 12 mm in length were cut from the slivers and used to provide a link with previous studies [1,3,13] that have focused on the use of sisal reinforcement in the strand form. Sisal field by-product, cleaned by rotary sieving, was provided by the Associação dos Pequenos Agricultores do Município de Valente (Apaeb), Brazil. This residual fibre has no market value and a quantity three times that of the commercial fibre consumed by the cordage industry remains in the fields.

The low-temperature thermomechanical (TMP) and chemi-thermomechanical (CTMP) pulping procedures employed were in keeping with the recommendations of Higgins [14] and Ramos et al. [15]. Slivers of the commercial and by-product sisal were initially cut to 30 mm in length and soaked for at least 16 h in tap water. In the case of CTMP, the chemical pre-treatment step consisted of boiling the strands in a 10% lime (on strand mass) liquor for a period of 1 h on completion of the soak.

Defibration was performed in an Asplund type D laboratory defibrator. Pre-steaming (120 s) and subsequent defibration (90 s) of each strand batch in the TMP and CTMP processes were carried out in saturated steam at temperatures of 130 and 121 °C, respectively. These conditions were selected on the basis of Higgins' [14] observation that well fibrillated softwood fibres could be obtained from the CTMP process at lower temperatures (in the vicinity of 130 °C), whereas smooth, lignin encased fibres were produced at higher temperatures (135–175 °C).

The pulps were post-refined by being passed several times through a Bauer 200 mm laboratory disc refiner fitted with straight-patterned "rubbing" plates. Detailed information regarding the mechanical refinement is in preparation for later publication. The refined pulps were passed through a 0.23 mm slotted Packer screen, vacuum de-watered, pressed, crumbed and stored in sealed bags under refrigeration.

The main physical properties of the TM and CTM pulps are summarised in Table 1. The Canadian Standard Freeness (CSF) of each pulp was determined in accordance with AS 1301.206s-88. CSF is an arbitrary measure of the drainage properties of pulp suspensions and is associated with the initial drain rate of the wet pulp pad during the de-watering process [16]. The low freeness values (less than 300 ml) are indicative of high degrees of external fibrillation of the fibres. These could lead to long drainage times during fibre–cement sheet production if a high mass fraction of fibre (e.g. 12%) were employed.

Fibre length was determined using a Galai WCIS-100 particle size analyser in the case of the commercial sisal TMP and CTMP, and a Kajaani FS-200 automated

Table 1
Pulp and fibre physical properties

Fibre	Process	Freeness (ml)	Fines (%)[a]	Length (mm)[b]	Transverse dimension (μm)[c]
Commercial	Strands	–	–	12	135
	TMP	224	2.34	2.25	10.2
	CTMP	5	3.88	2.46	12.7
By-product	CTMP	280	5.61	1.61	10.9

[a] Arithmetic basis.
[b] Length-weighted basis.
[c] Average of 20 determinations by SEM.

optical analyser in the case of the by-product sisal CTMP. Average length was calculated on a length-weighted basis, this being less influenced by the portion of fines (particles with less than 0.20 mm in length). Eq. (1) defines the calculation of length-weighted average (L) as described by Carvalho et al. [17]:

$$L = \sum n_i l_i^2 / \sum n_i l_i \quad (1)$$

where n_i = number of fibres in the ith class; l_i = mean length in the ith class.

The value of L is not only related to the average fibre length, but also to the length distribution. In the present study on pulped fibres it is reasonable to calculate the length-weighted average length to differentiate fibre fractions in accordance with their influence on composite properties. It is particularly interesting when analysing mechanical pulps that are expected to contain a large amount of fines with low capability of reinforcement [18].

2.3. Composite preparation

Natural fibre reinforced cement composites with fibre mass fractions ranging from 4% to 12% were prepared in the laboratory by a slurry vacuum de-watering technique. Plain OPC matrix was produced as a control using the same procedure. In the case of formulations incorporating 8% and 12% of fibre, matrix materials were added to the appropriate amount of moist fibres, pre-dispersed in water, to form a slurry of approximately 20% solids by mass. For formulations incorporating 4% fibre, a slurry of about 30% solids was used to minimise material segregation during de-watering. A slurry of 65% solids content was used for the production of neat OPC matrix. After stirring for 5 min using a high-speed laboratory mixer, the slurry was rapidly transferred to an evacuable 125×125 mm casting box. An initial vacuum of between 60 and 80 kPa (gauge) was applied until the bulk of the excess water was removed and a solid surface formed. The moist pad was tamped flat and vacuum was re-applied for 2 min. The consolidated pad was then removed from the casting box, transferred to an oiled steel plate and a fine wire mesh placed on top. Three pads per composite formulation were prepared in this manner, stacked on top of each other and pressed simultaneously at 3.2 MPa for 5 min. On completion of press consolidation, the plates and meshes were removed and the pads sealed in a plastic bag to cure in saturated air at room temperature.

Composites reinforced with sisal strand were produced by mixing the components for 5 min in a heavy-duty dough mixer at a 0.40 water–cement ratio, followed by de-watering and subsequent steps as described above. A composite strand content of 4% by mass was used as this had previously been found to be close to the practical limit for homogeneous distribution within the matrix [13].

After 7 days, the pads were removed from the bags and three 125×40 mm flexural test specimens were wet diamond sawn from each pad. Specimen depth was the thickness of the pad, which was around 6 mm. The specimens were then allowed to air cure in an environment of 23 ± 2 °C and $50 \pm 5\%$ relative humidity until tested at a total age of 28 days.

2.4. Mechanical and physical test methods

Nine flexural specimens were tested in three-point bending for each composite formulation. Modulus of rupture (MOR), modulus of elasticity (MOE) and fracture toughness (FT) values were determined. A span of 100 mm and a deflection rate of 0.5 mm/min were used for all tests on an Instron 1185 universal testing machine. FT was defined as the fracture energy divided by the specimen cross-sectional area. Fracture energy was calculated by integration of the load–deflection curve to the point where the load had dropped to 50% of its maximum value. Water absorption, bulk density and void volume values were obtained from six tested flexural specimens following the procedures specified in ASTM C 948-81. Results were subjected to one-way analysis of variance using Tukey's multiple comparison method to determine the significance of observed differences between sample means at the 95% confidence level ($\alpha = 0.05$).

2.5. Microscopy methods

Specimens from composites were analysed using a Philips XL30 field emission gun scanning electron microscope (SEM). Back-scattered electron (BSE) images were obtained from cut and polished surfaces. BSE images permit the identification of composite phases by way of their shape or grey-scale, elements with higher atomic numbers appearing lighter and therefore being easily differentiated from cellulose fibres or pores. Energy dispersive X-ray spectroscopy (EDS) analysis was carried out on the specimens to provide a semi-quantitative determination of chemical elements. Preparation of the specimens consisted of their impregnation with epoxy resin and progressive smoothing, a final diamond polishing paste grade of 0.1 μm being used, as detailed by Savastano and Agopyan [13]. The specimens were then provided with a light carbon coating. It should be noted that composite microstructures were examined at ages greater than 28 days and some changes from those existing at the time of testing would be expected to have occurred.

3. Mechanical and physical results

The mean values and associated standard deviations of the mechanical properties of the various composites are shown in Figs. 1–3. Fig. 1 depicts MOR and FT values for OPC reinforced with commercial sisal TMP and BFS reinforced with by-product sisal CTMP. Fibre content was varied from 4% to 12% by mass. The composites reached their maximum flexural strengths of 18–20 MPa at fibre contents about 8%. These strengths represent an improvement of at least 58% over that of the neat OPC matrix. BFS reinforced by 12% of by-product sisal possessed an outstanding FT value of 1.6 kJ/m^2, more than 40 times that of the non-reinforced material, but at the cost of a considerable loss in strength.

There is a general relationship between strength and toughness that is associated with fibre–matrix bonding. The stronger the interfacial bond the greater the strength but the lesser the FT. This behaviour with re-

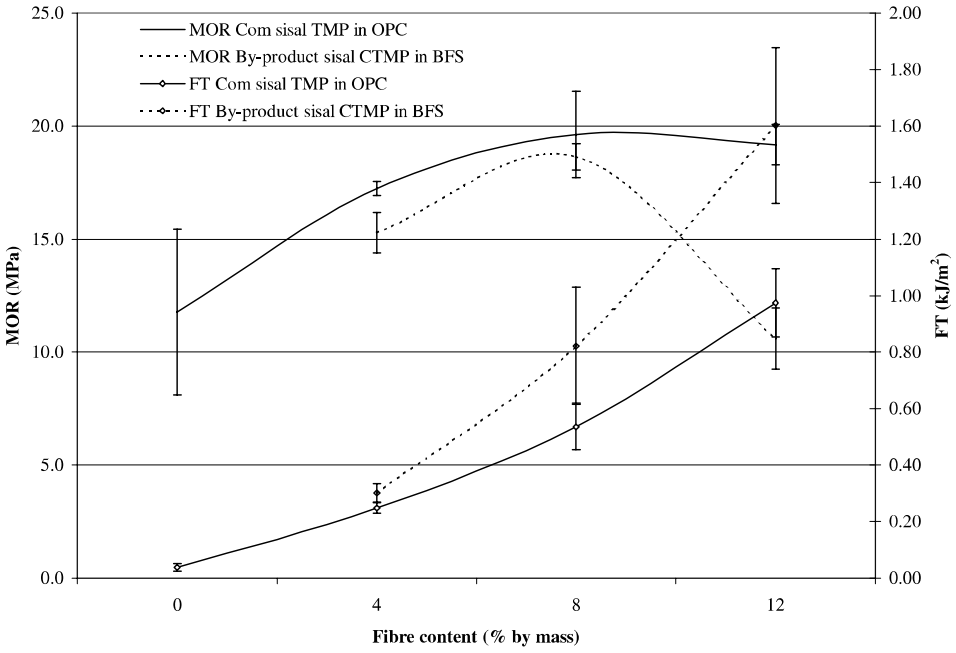

Fig. 1. Variation of MOR and FT with fibre content of the composites at 28 days.

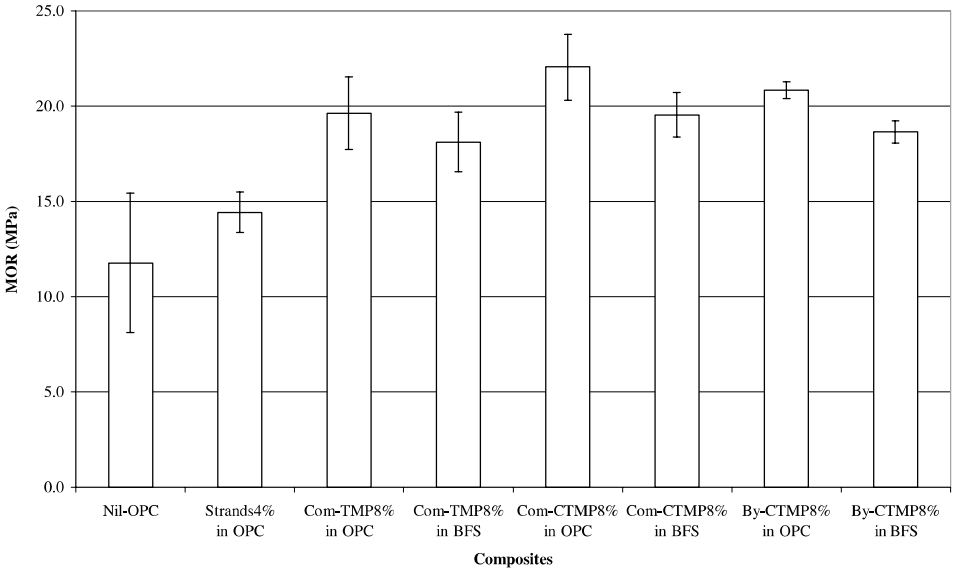

Fig. 2. MOR of several 8% pulp fibre–cements, plain matrix and 4% strand fibre–cement.

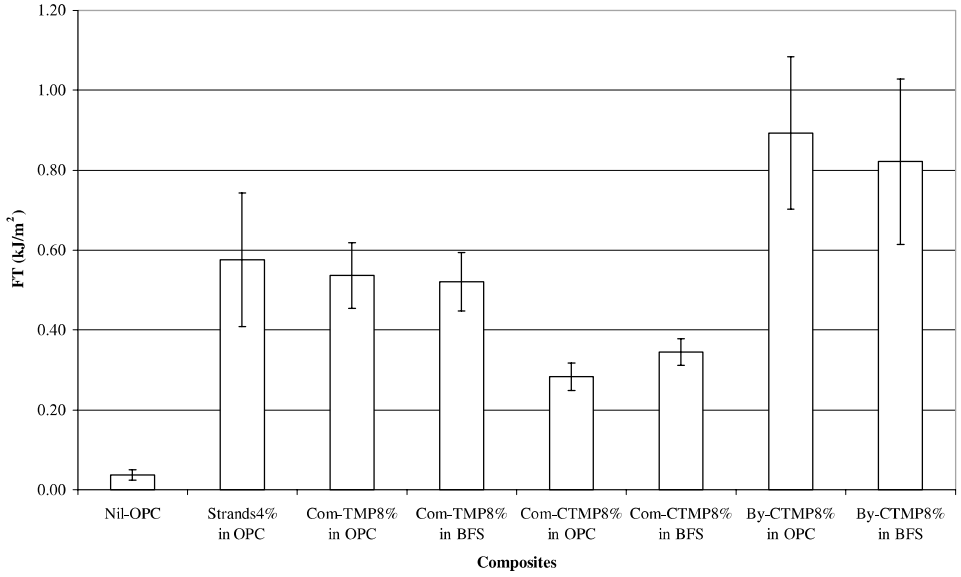

Fig. 3. FT of several 8% pulp fibre–cements, plain matrix and 4% strand fibre–cement.

spect to FT results from an increased incidence of fibre fracture and corresponding decrease in the energy absorbed through fibre pullout processes [19].

The by-product CTMP consisted of shorter, lower aspect ratio (length/transverse dimension) fibres than the pulps of commercial sisal (Table 1), contributing to a higher incidence of fibre pullout and consequently to a greater dissipation of frictional energy as suggested by Coutts [20]. The by-product pulp also appeared to retain a higher amount of non-fibrous components (e.g. extractives and pithy material) as, in part, indicated its fines content. These extraneous materials may have interfered with the hydration of the BFS in the neighbourhood of the fibres, preventing effective stress transfer and, at the higher fibre contents, contributing to the significant decrease in flexural strength. A similar behaviour was reported by Savastano et al. [21] for OPC-based paste reinforced with by-product sisal and banana fibres.

Fig. 2 depicts the strengths of several composites containing 8% by mass of pulped cellulose fibre. Similar strengths were obtained in OPC- and BFS-based matrices, 8% pulp providing significantly ($p < 0.05$) better reinforcement than 4% of 12 mm long chopped strand fibre in the OPC matrix. However, the use of the vacuum de-watering and pressing procedures contributed to a better performance of the strand reinforced composites than was achieved in a previous study by Savastano and Agopyan [22]. In the earlier study, which used conventional dough-mixing and compaction by vibration, flexural strengths of less than 4 MPa were obtained.

The ageing effect in strand reinforced OPC has been shown to be a major limitation of these materials [3,9]. Since individual filaments within strands are linked to each other by lignin, which is readily decomposed in alkali media, a considerable decrease in the mechanical properties of cement-based materials reinforced with natural fibres in this form can be expected during a relatively short lifetime.

Pulping processes separate the fibres in the strands prior to their incorporation in the matrix, and may reduce lignin levels below those of the original strand fibres. Pulped fibres are potentially more resistant to cement attack as already shown in another work [10] where composites were prepared by the same slurry dewatering method used in this study. In the referenced work, BFS-based matrix with cellulose fibre maintained or even increased its tenacity after 1 year under natural weathering in comparison with the short-term (28 days) behaviour.

Fig. 3 illustrates the low FT of composites containing 8% by weight of commercial sisal CTMP. The low value is assumed to be the result of superior fibre–matrix bonding leading to a predominance of fibre fracture rather than pull-out during the failure process as already discussed in this section and elsewhere [19,23]. By-product sisal CTMP had a superior behaviour as discussed previously and chopped strands also produced an acceptable level of energy dissipation due to their low aspect ratio (~90).

Coutts and Warden [2] reported flexural strengths up to 18 MPa and FT values of 2.6 kJ/m^2 for air-cured cement composites containing 8% by mass of chemically pulped sisal. The superior ductility can be understood as the result of optimised interfacial bonding occurring between the well pulped fibres and the matrix, and a low incidence of non-cellulose components.

In agreement with other studies [2,24], MOE decreased with an increase in fibre content, irrespective of the type of binder used. This behaviour can be explained

Table 2
Physical properties of composites

Fibre		Binder	Water absorption (% by mass)	Bulk density (g/cm^3)	Permeable voids (% by volume)
Type	Content (% by mass)				
Nil strands	–	OPC	10.7 ± 0.5	2.18 ± 0.03	23.4 ± 0.8
Strands	4	OPC	14.9 ± 0.7	1.86 ± 0.04	27.8 ± 0.8
Commercial sisal	4	OPC	18.7 ± 0.7	1.68 ± 0.02	31.4 ± 0.8
TMP	8	OPC	22.5 ± 0.8	1.54 ± 0.02	34.6 ± 0.8
	12	OPC	26.3 ± 0.9	1.44 ± 0.02	37.8 ± 0.9
	8	BFS	31.0 ± 0.5	1.37 ± 0.01	42.3 ± 0.4
Commercial sisal	8	OPC	21.8 ± 0.4	1.62 ± 0.01	35.2 ± 0.5
CTMP	8	BFS	29.4 ± 0.5	1.45 ± 0.01	42.5 ± 0.5
By-product sisal	8	OPC	21.1 ± 1.2	1.54 ± 0.02	32.4 ± 1.4
CTMP	4	BFS	26.0 ± 0.4	1.52 ± 0.01	39.4 ± 0.2
	8	BFS	30.0 ± 0.7	1.39 ± 0.02	41.8 ± 0.4
	12	BFS	36.8 ± 0.7	1.26 ± 0.02	46.3 ± 0.3

Listed are average values and standard deviations.

by the lower modulus of the fibre when compared with the matrix, incorporation of air during production and a decrease in packing efficiency at higher fibre contents (see Table 2). In comparison with the MOE of 23.5 GPa of the OPC matrix, a 44% reduction was found for the composite containing 4% commercial sisal TMP. With increasing amounts of the same reinforcement, the MOE followed the same tendency but at a lower rate, falling to a value of 7.1 GPa at 12% fibre content. At a fibre content of 8%, MOE was around 11 GPa for the OPC matrix reinforced with either TMP or CTMP fibres; reinforcement by the same amount of pulps resulted in an MOE of about 7 GPa in BFS-based composites. The lower stiffness of the BFS-based composites can be related to their physical properties (Table 2), i.e. the water absorption and porosity of BFS composites being significantly higher than the corresponding OPC composites. Such performances could be due to insufficient hydration levels of the BFS-based cement [25].

Water absorption, bulk density and permeable void volume are related to each other, as reflected by Table 2, and to mechanical performance as already commented on. Composites with a 12% fibre content revealed densities around 1.3–1.4 g/cm^3, suggesting potential applications as lightweight materials. However, their water absorption values were correspondingly high. At a 4% content, TMP fibres led to greater permeability in the OPC matrix than did strand fibres as a consequence of the presence of a significantly higher number of individual filaments resulting in a more extensive network of interconnected voids.

4. Microstructure properties

Fig. 4 shows a transverse section of an approximately 100 μm wide sisal strand in a polished OPC surface. A high degree of matrix porosity (medium grey area) and microcracking can be seen in its immediate vicinity, in contrast to the bulk matrix. Square 1 and rectangle 2 in the micrograph indicate the target regions of the two EDS analyses that follow in Figs. 5 and 6. The EDS analyses show a significant presence of Ca, Si, S and Al but no indication of a predominance of calcium hydroxide (portlandite). The presented behaviour differs from that reported by Savastano and Agopyan [13] for natural strand fibres in OPC paste. These authors observed porous transition zones, up to 100 μm thick, rich with portlandite crystals. The different aspect and composition of the transition zone in the present work is in agreement with [8] and can be considered a result of the vacuum de-watering/press consolidation production method employed.

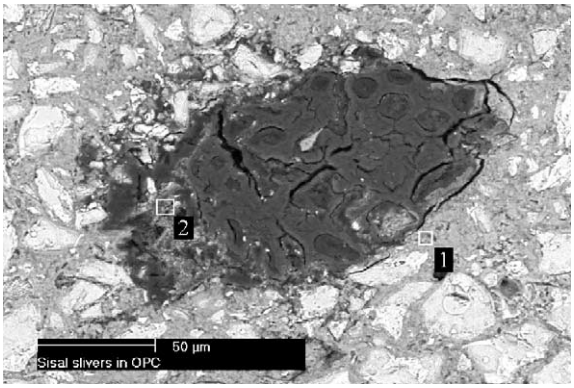

Fig. 4. BSE image of 149 days old 4% sisal strand reinforced OPC. Transition zone between the macro-fibre and the cement-based matrix.

BFS containing 8% commercial sisal CTMP is shown in Fig. 7 at a similar magnification to that used for Fig. 4. Several pulped filaments can be seen in arbitrary position. The elongated shape combined with the narrowed lumen is indicative of the mechanical refining to which they were subjected. The collapsed, ribbon-like

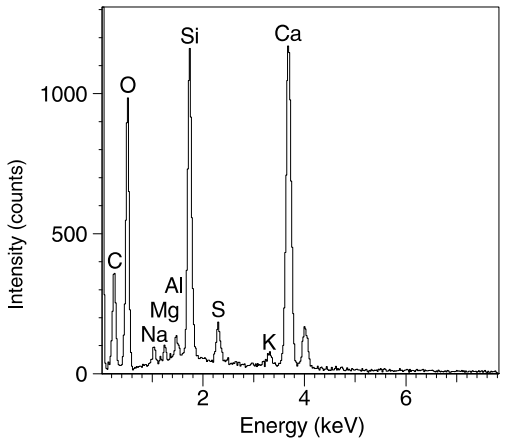

Fig. 5. EDS spectrum of an interfacial area between a sisal strand and OPC matrix (square 1 in Fig. 4).

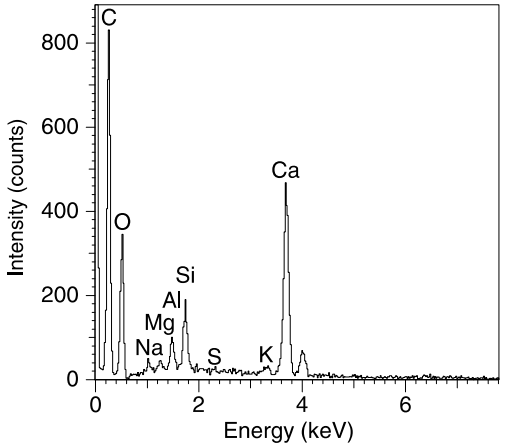

Fig. 6. EDS spectrum of a second interfacial region between a sisal strand and OPC matrix (rectangle 2 of Fig. 4).

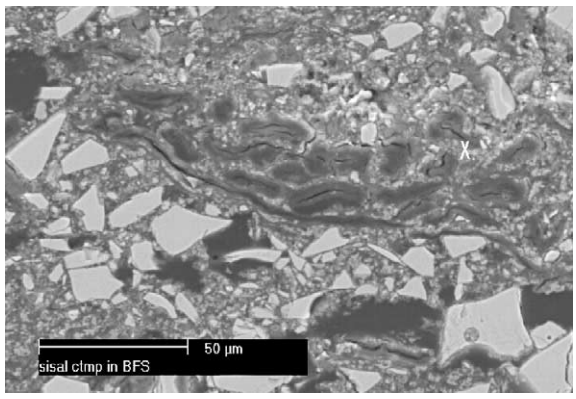

Fig. 7. BSE image of 61 days old 8% commercial sisal CTMP in BFS. Ribbon-like filaments appear in arbitrary position in the central area of the micrograph. 'X' indicates the region used for EDS analysis and shown in Fig. 8.

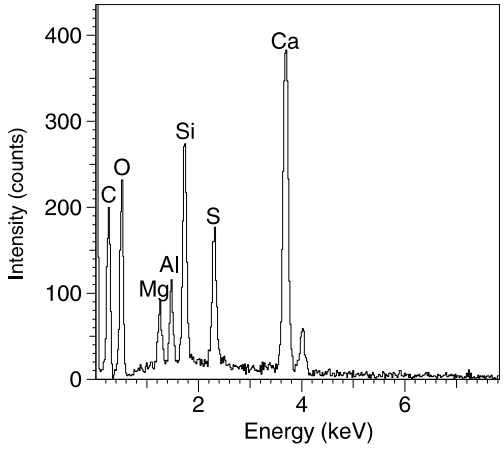

Fig. 8. EDS spectrum of matrix region between two fibres.

fibre could be expected to lead to improved fibre–matrix bonding and also occasional fibre–fibre bonding, to be more conformable [26] and hence to allow optimum packing of the composites during fabrication. EDS analysis of the region denoted by the 'X' in Fig. 7 revealed a typical composition for cement hydration products with no pre-eminence of the calcium element (Fig. 8). The chemical elements of significance in the analysis (Ca, Si, S, Al and Mg) are in accordance with the presented composition of anhydrous BFS plus activators.

Fig. 9 shows a general view at low magnification of residual sisal CTMP in OPC matrix. A content of 4% was selected for examination to facilitate observation of the fibres (medium grey regions) into the matrix. The high specific area of contact accomplished with pulped fibres, allied to the predominance of 2D distribution of such fibres in thin elements (a consequence of the production technique described in Section 2.3), contribute to improved stress transfer and also to porous interconnection with a remarkable influence on the macrostructural performance of the composite material.

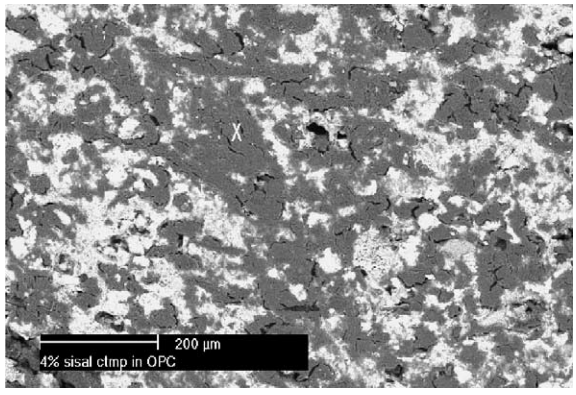

Fig. 9. BSE image of 65 days old 4% by-product sisal CTMP in OPC. General view of the composite with fibres (medium grey) and pores (dark grey) dispersed in the cement matrix (light grey). 'X' indicates linked fibres.

Instances of heterogeneous fibre distribution as a result of fibre bundle formation can be observed in the image.

5. Conclusion

Air-cured cement matrices reinforced with TMP or CTMP fibres obtained from commercial and by-product sisal strands demonstrated acceptable mechanical behaviour at 28 days of age in comparison with similar works reported in the literature [5,27,28]. The addition of 12% by mass of fibre to a BFS matrix provided up to a 43-fold increase in FT when compared to the brittle OPC paste used as a control. The MOR of OPC-based composites reached 22 MPa, a more than 5-fold increase over the results obtained in previous studies with similar materials. At a fibre content of 8%, the OPC composite's MOE was approximately 11 GPa and the water absorption around 22% by mass; at the same fibre content, the MOE of the BFS composites was about 7 GPa, and the water absorption 30% by mass, irrespective of the type of pulp used as reinforcement.

The use of pulped filaments and the slurry de-watering/press consolidation method of composite fabrication, leading a large contact surface area of high quality, were the main reasons for the improved properties of the fibre–cements studied at initial ages. Analysis of their microstructures confirmed good adhesion between the phases and revealed an absence of the thick, highly porous interfacial areas and portlandite concentrations that have been observed in related strand fibre reinforced materials based on OPC.

Such an effective combination of techniques and alternative raw-materials was an initial approach in the short-term to non-conventional fibre–cements. This study encourages further and structured research toward the development of commercial products with suitable long-term performance, based either on strength or on toughness, for popular housing in developing countries.

Acknowledgements

The authors would like to thank the Fundação de Amparo à Pesquisa do Estado de São Paulo (Fapesp) and the Conselho Nacional de Desenvolvimento Científico e Tecnológico (CNPq), Brazil, for their financial support; and Allyson Pereira and Göran Längfors of CSIRO Forestry and Forest Products for their skilful assistance. Thanks also to John V. Ward and Mark Greaves of the CSIRO Forest Products Laboratory for providing access to microscopy facilities and guidance in their effective use.

References

[1] Guimarães SS. Vegetable fiber–cement composites. In: Sobral HS, editor. Proceedings of the Second International RILEM Symposium on Vegetable Plants and their Fibres as Building Materials. London: Chapman and Hall; 1990. p. 98–107.
[2] Coutts RSP, Warden PG. Sisal pulp reinforced cement mortar. Cem Concr Compos 1992;14(1):17–21.
[3] Tolêdo Filho RD, Scrivener K, England GL, Ghavami K. Durability of alkali-sensitive sisal and coconut fibres in cement mortar composites. Cem Concr Compos 2000;22(2):127–43.
[4] Oliveira CTA, John VM, Agopyan V. Pore water composition of activated granulated blast furnace slag cements pastes. In: Proceedings of the Second International Conference on Alkaline Cements and Concretes. Kiev: Kiev State Technical University of Construction and Architecture; 1999. p. 9.
[5] Eusebio DA, Cabangon RJ, Warden PG, Coutts RSP. The manufacture of wood fibre reinforced cement composites from *Eucalyptus pellita* and *Acacia mangium* chemi-thermomechanical pulp. In: Proceedings of the Fourth Pacific Rim Bio-Based Composites Symposium. Bogor: Bogor Agricultural University; 1998. p. 428–36.
[6] Balaguru P, editor. Thin reinforced concrete products and systems. Detroit: ACI; 1994. p. 25–42 (SP-146-3).
[7] Mindess S. Fibre reinforced concrete: challenges and prospects. In: Banthia N, Mindess S, editors. Fibre reinforced concrete. Vancouver: University of British Columbia; 1993. p. 1–11.
[8] Coutts RSP. Fibre–matrix interface in air-cured wood-pulp fibre–cement composites. J Mater Sci Lett 1987;6(2):140–2.
[9] Gram H-E. Durability of natural fibres in concrete. In: Swamy RN, editor. Natural fibre reinforced cement and concrete. Glasgow: Blackie; 1988. p. 143–72.
[10] Savastano Jr H, Warden PG, Coutts RSP. Performance of low-cost vegetable fibre–cement composites under weathering. In: Duncan J, editor. Proceedings of the CIB World Building Congress. Wellington: Branz/CIB; 2001. p. 11 (CD Rom, paper number 108).
[11] MacVicar R, Matuana LM, Balatinecz JJ. Aging mechanisms in cellulose fiber reinforced cement composites. Cem Concr Compos 1999;21(3):189–96.
[12] John VM, Agopyan V, Derolle A. Durability of blast furnace-slag-based cement mortar reinforced with coir fibres. In: Sobral HS, editor. Proceedings of the Second International RILEM Symposium on Vegetable Plants and their Fibres as Building Materials. London: Chapman and Hall; 1990. p. 87–97.
[13] Savastano Jr H, Agopyan V. Transition zone studies of vegetable fibre–cement paste composites. Cem Concr Compos 1999;21(1): 49–57.
[14] Higgins HG. Paper physics in Australia. CSIRO Division of Forestry and Forest Products, Melbourne, 1996.
[15] Ramos J, Davalos F, Navarro F. High yield pulping from sugar cane bagasse and other non-wood plant fibers, an state of the art review. In: Proceedings of the Nanjing International Symposium on High Yield Pulping. Nanjing: Chinese Academy of Forestry; 1997. p. 152–86.
[16] Coutts RSP, Ridikas V. Refined wood fibre–cement products. Appita 1982;35(5):395–400.
[17] Carvalho MG, Ferreira PJ, Martins AA, Figueiredo MM. A comparative study of two automated techniques for measuring fiber length. Tappi J 1997;80(2):137–42.
[18] Bichard W, Scudamore P. An evaluation of the comparative performance of the Kajaani FS-100 and FS-200 fiber length analyzers. Tappi J 1988;71(12):149–55.

[19] Coutts RSP, Kightly P. Bonding in wood fibre–cement composites. J Mater Sci 1984;19:3355–9.
[20] Coutts RSP. Sticks and stones . . .!! Forest Products Newsletter. CSIRO Div Chem Wood Technol 1986;2(1):1–4.
[21] Savastano Jr H, Warden PG, Coutts RSP. Brazilian fibres as reinforcement for cement-based composites. Cem Concr Compos 2000;22(5):379–84.
[22] Savastano Jr H, Agopyan V. Transition zone of hardened cement paste and vegetable fibres. In: Swamy RN, editor. Proceedings of the Fourth International RILEM Symposium of Fibre Reinforced Cement and Concrete. London: E & FN Spon; 1992. p. 1110–9.
[23] Sarigaphuti M, Shah SP, Vinson KD. Shrinkage cracking and durability characteristics of cellulose fiber reinforced concrete. ACI Mater J 1993;90(4):309–18.
[24] Soroushian P, Shah Z, Won J-P. Optimization of wastepaper fiber–cement composites. ACI Mater J 1995;92(1):82–92.
[25] Swamy RN. Design for durability and strength through the use of fly ash and slag in concrete. In: Malhotra VN, editor. Proceedings of the Third CANMET/ACI International Conference on Advances in Concrete Technology, Auckland. 1997. p. 1–72 (ACI International SP-171-1).
[26] McKenzie AW. A guide to pulp evaluation. Melbourne: CSIRO; 1994.
[27] Soroushian P, Marikunte S, Won J-P. Statistical evaluation of mechanical and physical properties of cellulose fiber reinforced cement composites. ACI Mater J 1995;92(2):172–80.
[28] Shao Y, Moras S, Ulkem N, Kubes G. Wood fibre–cement composites by extrusion. Can J Civil Eng 2000;27(3):543–52.